

The black-hole masses of Seyfert galaxies and quasars

R.J. McLure¹ & J.S. Dunlop²

¹*Nuclear and Astrophysics Laboratory, University of Oxford, Keble Road, Oxford, OX1 3RH*

²*Institute for Astronomy, University of Edinburgh. Royal Observatory, Edinburgh EH9 3HJ.*

Submitted for publication in MNRAS

ABSTRACT

The central black-hole masses of a sample of 30 luminous quasars are estimated using H_β FWHM measurements from a combination of new and previously-published nuclear spectra. The quasar black-hole mass estimates are combined with reverberation-mapping measurements for a sample of Seyfert galaxies (Wandel, Peterson & Malkan 1999) in order to study AGN black-hole masses over a wide range in nuclear luminosity. The link between bulge luminosity and black-hole mass is investigated using two-dimensional disc/bulge decompositions of the host-galaxy images, the vast majority of which are high resolution HST observations. It is found that black-hole mass and bulge luminosity are well correlated and follow a relation consistent with that expected if black-hole and bulge mass are directly proportional. Contrary to the results of Wandel (1999) no evidence is found that Seyfert galaxies follow a different $M_{\text{bh}} - M_{\text{bulge}}$ relation to quasars. However, the black-hole mass distributions of the radio-loud and radio-quiet quasar sub-samples are found to be significantly different, with the median black-hole mass of the radio-loud quasars a factor of three larger than their radio-quiet counterparts. Finally, utilizing the elliptical galaxy fundamental plane to provide stellar velocity dispersion estimates, a comparison is performed between the virial H_β black-hole mass estimates and those of the $M_{\text{bh}} - \sigma$ correlations of Gebhardt et al. (2000a) and Merritt & Ferrarese (2000). With the disc geometry of the broad-line region adopted in this paper, the virial H_β black-hole masses indicate that the correct normalization of the black-hole vs. bulge mass relation is $M_{\text{bh}} \simeq 0.0025 M_{\text{bulge}}$, while the standard assumption of purely random broad-line velocities leads to $M_{\text{bh}} \simeq 0.0008 M_{\text{bulge}}$. The normalization of $M_{\text{bh}} \simeq 0.0025 M_{\text{bulge}}$ provided by the disc model is in remarkably good agreement with that inferred for our quasar sample using the (completely independent) $M_{\text{bh}} - \sigma$ correlations.

Key words: galaxies: active – galaxies: nuclei – galaxies: Seyfert – quasars: general

1 INTRODUCTION

The evidence that supermassive black-holes are ubiquitous in nearby inactive galaxies is now extremely strong (eg. van der Marel 1999, Kormendy & Richstone 1995). Furthermore, several studies have concluded that the masses of these dormant black-holes are directly proportional to the mass of the galaxy bulge (spheroidal) component (eg. Kormendy & Richstone 1995, Magorrian et al. 1998). Although a significant scatter is present in the correlation ($\Delta M_{\text{bh}} \simeq 0.5$ dex at a given bulge mass), the data appear to suggest that $M_{\text{bh}} = (0.002 \rightarrow 0.006) M_{\text{bulge}}$. While studies of nearby inactive galaxies have seen a reasonably coherent picture emerge, the situation with regard to active galaxies is less certain. Although the black-hole mass relation observed in nearby inactive galaxies can be comfortably reproduced by combined galaxy+quasar formation models (eg. Wilman,

Fabian & Nulsen 2000, Kauffmann & Haehnelt 2000), observational studies to investigate the form of the $M_{\text{bh}} - M_{\text{bulge}}$ relation in active galaxies have led to seemingly contradictory results.

In a study of the $M_{\text{bh}} - M_{\text{bulge}}$ relation in quasars, Laor (1998) used the FWHM of the broad H_β emission line, together with a calibration between the broad-line region (BLR) radius and quasar UV luminosity, to obtain virial black-hole mass estimates for 14 PG quasars. Using estimates of the host-galaxy bulge luminosities from the HST study of Bahcall et al. (1997), Laor found a $M_{\text{bh}} - L_{\text{host}}$ correlation which agreed reasonably well with the results of Magorrian et al. (1998). In contrast, Wandel (1999) found that virial black-hole mass estimates for a sample of 17 Seyfert1 galaxies, based on the H_β FWHM and reverberation mapping measurements of the BLR radius, were substantially smaller than would be expected from the $M_{\text{bh}} - M_{\text{bulge}}$

arXiv:astro-ph/0009406v3 7 Jun 2001

relation seen in nearby inactive galaxies. Using estimates of the Seyfert galaxy bulge luminosities from the empirical morphology-based formula of Simien & de Vaucouleurs (1986), Wandel found that $M_{\text{bh}}/M_{\text{bulge}} \sim 10^{-3.5}$, a factor of between ten and twenty lower than found for both nearby inactive galaxies (Magorrian et al. 1998) and for luminous quasars (Laor 1998).

The implication of the Wandel (1999) result is that there exists a difference in the formation or triggering mechanism at work in Seyfert galaxies and quasars. This possibility is explored by Wang, Biermann & Wandel (2000) who present a model in which $M_{\text{bh}}/M_{\text{bulge}} \propto \sigma^{1.4}$, where σ is the velocity dispersion of the accreting gas. In this model the high values of $M_{\text{bh}}/M_{\text{bulge}}$ found in quasars and nearby bulges are the asymptotic, high-velocity case, possibly produced by a violent merger event. In contrast, the much lower ratios found in Seyfert galaxies are the result of the accretion of lower velocity gas triggered by tidal disruption.

In this paper the $M_{\text{bh}} - M_{\text{bulge}}$ relation is examined over a wide range in AGN luminosity by combining new results for a sample of 30 luminous ($M_V < -23$) quasars with a re-analysis of the bulge masses attributed to the Wandel (1999) Seyfert galaxy sample. First, in Section 2 we briefly review the complications and potential uncertainties in deriving black-hole mass estimates from emission-line widths, and explore how best to model the geometry of the broad-line region for the purpose of black-hole estimation in AGN. Next, in Section 3 we describe the sample of objects selected for study, present the new spectroscopic observations, and explain how reliable bulge luminosities have been extracted from existing HST images. In Section 4 three important questions are addressed. Firstly, do powerful AGN actually display a $M_{\text{bh}} - M_{\text{bulge}}$ correlation consistent with that found in nearby inactive galaxies? Secondly, do the apparent differences between Seyfert galaxies and quasars actually stem from fundamental differences between the two AGN classes, or simply from systematic errors in estimating Seyfert bulge luminosities? And finally, do differences in black-hole mass and gas accretion rates play a crucial role in determining the radio properties of AGN? In Section 5 stellar velocity estimates for a sub-sample of the quasars are used to compare our virial $H\beta$ black-hole mass estimates with those of the $M_{\text{bh}} - \sigma$ relations discovered by Gebhardt et al. (2000a) and Merritt & Ferrarese (2000). Finally, our main conclusions are summarized in Section 6. Unless otherwise specified all cosmological calculations performed in this paper assume $H_0 = 50 \text{ kms}^{-1} \text{ Mpc}^{-1}$, $q_0 = 0.5$ and $\Lambda = 0$.

2 THE VIRIAL BLACK-HOLE MASS ESTIMATE

The basic theory of obtaining virial black-hole mass estimates from quasar emission lines has been discussed extensively in the literature (eg. Wandel, Peterson & Malkan 1999) and consequently only a brief outline is provided here. The underlying assumption is that the broad emission lines are produced by material which is gravitationally bound and orbiting with keplerian velocities. If this assumption is applicable then an estimate of the central mass is given by $M_{\text{bh}} = R_{\text{BLR}} V^2 G^{-1}$, where R_{BLR} is the radius of the BLR and V is the velocity of the line-emitting material. There

are two standard methods of estimating the radius of the broad-line region. The first of these, and presumably the more accurate, is to use the time delay between continuum and line variations. For the sample of Seyfert galaxies studied by Wandel, Peterson & Malkan (1999) and Wandel (1999), long-term monitoring has provided such reverberation mapping estimates of the radius of the broad-line region. In the absence of reverberation mapping data for the quasar sample it is necessary to use a more indirect estimate of the broad-line radius. The method used here is the correlation between R_{BLR} and monochromatic luminosity at 5100\AA found by Kaspi et al. (2000), from their reverberation mapping results for 17 PG quasars. When converted to the cosmology adopted in this paper, the Kaspi et al. correlation becomes:

$$R_{\text{BLR}} = 18.65 \left(\frac{\lambda L_{\lambda}(5100\text{\AA})}{10^{37} W} \right)^{0.7} \text{lt} - \text{days} \quad (1)$$

The other necessary component for the virial mass estimate is a measure of velocity of the line emitting material. To obtain this, Wandel (1999) adopted the assumption of random orbits, in which case $V = \frac{\sqrt{3}}{2} \text{FWHM}$. However, the assumption of random orbits seems unrealistic for quasars. In particular, for radio-loud quasars where the radio core:lobe ratio provides an independent measure of orientation, there exists strong evidence that the velocity-field of the broad-line region is better represented by a combination of a random isotropic component, with characteristic velocity V_r , and a component only in the plane of the disk, with characteristic velocity V_p (Wills & Browne 1986).

In this case, the observed FWHM will be given by

$$\text{FWHM} = 2(V_r^2 + V_p^2 \sin^2 \theta)^{1/2} \quad (2)$$

where θ is the angle between the disc normal, and the line of sight to the observer. In the case of radio-quiet objects we have no guide as to what precise value of θ should be adopted for a particular object. However, attempts to unify radio-loud quasars and galaxies (e.g. Barthel 1989), and imaging polarimetry studies of radio-quiet AGN (e.g. Antonucci & Miller 1985) support a picture in which an active nucleus is likely to appear to the observer as a quasar provided $\theta < 45^\circ$.

In order to test the viability of this disc-model we have attempted to reproduce the form of the cumulative FWHM distribution of the combined quasar+seeyfert sample. As can be seen from Fig 1b., the cumulative distribution of the data is convex in shape. This form of distribution cannot in fact be produced by a single disc model in which the angle between the disc normal and observer's line of sight is assumed to be randomly distributed between $\theta = 0$ and some adopted upper limit $\theta = \theta_{\text{max}}$. The reason for this is simply that, given a random distribution of theta (and V_p significantly larger than V_r) the cumulative distribution of FWHM grows proportional to solid angle $1 - \cos \theta$.

However, we have found that the form of the observed distribution can in fact be almost perfectly reproduced by a model which includes only one additional free parameter. Specifically we have relaxed the assumption of a purely random distribution of theta for $\theta < \theta_{\text{max}}$ by exploring whether the data can be described by a combination of two randomly-oriented disc-model populations with the same characteristic orbital velocity but different angular constraints. The best-fitting model parameters were found to be $V_p = 5500$

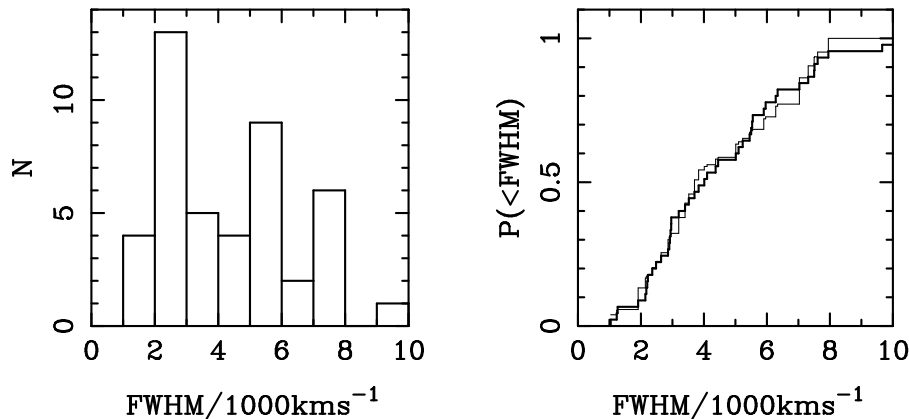


Figure 1. The left-hand panel shows the distribution of H_β FWHM measurements for the 45 objects in the combined quasar+seiyfert sample. The right-hand panel shows the cumulative FWHM distributions displayed by the data (thick line) and that of the disc BLR model discussed in the text (thin line). The two cumulative distributions can be seen to be extremely similar, with the KS test probability of $p = 0.99$ showing them to be statistically indistinguishable.

kms^{-1} , $\theta_{\max}(1) = 46^\circ$, $\theta_{\max}(2) = 20^\circ$, with the two models contributing 58% and 42% of the combined model distribution respectively. In both cases the model AGN are assumed to lie randomly at angles between $0 < \theta < \theta_{\max}$ to the line of sight. Although two-component disc-models with non-zero random velocity components and independent orbital velocity components were considered, it was found that the introduction of these extra free parameters did not produce significantly improved fits. The best-fitting model distribution is shown as the thin line in Fig 1b. and can be seen to be an excellent representation of the data, with an application of the Kolmogorov-Smirnov test showing the two distributions to be indistinguishable ($p = 0.99$). By substituting the fitted model parameters into Eqn 2. it is now possible to determine the average relationship between observed FWHM and actual orbital velocity V_p by calculating $\langle \sin \theta \rangle$ as weighted by solid angle. We therefore find that on average $V_p = 1.5 \times \text{FWHM}$, and it is this relation which is adopted throughout the remainder of this paper.

As can be seen from the best-fitting parameters presented above, the dominant population of objects in this two-component disc model of the BLR is constrained to lie within $\sim 45^\circ$ to the line of sight, as expected in the unified model (eg. Barthel 1989). In contrast, the second population of objects is required to lie within a smaller range of angles to the line of sight than is normally assumed in the unified model (ie. $\sim 20^\circ$). However, one can argue that this is entirely reasonable given that the present sample is largely dominated by powerful, optically-selected broad-line AGN. However, it is worth noting the implications of the assumptions in this simple model, and the effect of relaxing them. Due to the fact that the virial black-hole mass estimate is proportional to V_p^2 , the adoption of the standard model in which BLR velocities are purely random ($V_p = 0.87 \times \text{FWHM}$) leads to black hole mass estimates three times *smaller* than derived in this paper. Further evidence in support of the appropriateness of the BLR model adopted here is discussed in Section 4.1 and Section 5.

3 THE SAMPLE, OBSERVATIONS AND DATA REDUCTION

The sample of 30 luminous quasars ($M_V < -23$) studied in this paper consists of two optically-matched sub-samples of 17 radio-quiet quasars and 13 radio-loud quasars. The unique feature of this sample is that all of its members have accurate bulge luminosities available from detailed two-dimensional modelling of HST images. Nineteen of the objects are taken from the sample studied by McLure et al. (1999) and Dunlop et al. (2000), with a further eleven taken from the sample of Bahcall et al. (1997). This is therefore the best dataset currently available for this type of investigation. The sample of Seyfert galaxies consists of fifteen of the seventeen objects studied by Wandel (1999). The two objects which are not included, Akn 120 & Mrk 110, have been excluded on the basis that no suitable HST archive data exists for these objects, and that a reliable disc/bulge decomposition could not be identified in the literature.

3.1 Nuclear spectra

The new observations presented in this paper consist of nuclear spectra of 13 of the quasar sample which were obtained in December 1999 on the 2.5m Isaac Newton Telescope on La Palma. All observations used the Intermediate Dispersion Spectrograph (IDS) with the 235mm camera and the EEV10 4096×2048 pixel CCD as the detector. Integration times on individual objects were ≥ 3000 seconds, with the RV300 grating providing spectra centred on 5800\AA with a resolution of $\simeq 4.5\text{\AA}$. At the average redshift of the quasar sample ($z \sim 0.2$) this ensured that the spectra were always approximately centred on the H_β line, with the wavelength coverage of $\sim 4000\text{\AA}$ allowing an accurate continuum determination.

The reduction of the spectra was performed in IRAF in the standard way, including flux calibration, and correction for atmospheric extinction and galactic reddening. The final wavelength calibrated spectra were interpolated onto a linear dispersion of $1.5\text{\AA}/\text{pix}$ and are shown in Fig 6.

The H_β FWHM measurements for 16/17 of the remaining

quasars in the sample are taken from the Boroson & Green (1992) and Corbin (1997) studies. Given that the H_β FWHM enters into the virial mass estimate quadratically, it is obviously important that there is no large systematic offset between the two sets of spectra. Fortunately, five of the quasars for which new spectra have been obtained also feature in the Boroson & Green study. For these five objects the FWHM values determined from the new spectra agree well with those of Boroson & Green, $\Delta\text{FWHM} = 10 \pm 4\%$, providing confidence that large variations in measured FWHM values do not introduce large systematic errors into the virial black-hole estimates. The H_β FWHM measurement for one final object, 1635+119, is taken from the spectrum of Wills & Browne (1986).

3.2 Host-galaxy bulge luminosities

A substantial effort has been invested in providing accurate estimates of the bulge luminosities for all the objects included in this study. All 30 objects in the quasar sample have bulge luminosities derived from two-dimensional modelling of HST data from the deep host-galaxy imaging studies of Dunlop et al. (2000) and Bahcall et al. (1997). The addition of the Dunlop et al. (2000) host-galaxy sample means that the number of quasars with reliable bulge luminosities is a factor of two greater than was available to Laor (1998).

Of equal importance to this study are revised estimates of the bulge luminosities within the Seyfert galaxy sample. The bulge luminosities used by Wandel (1999) were taken from Whittle (1992) and are based upon an application of the Simien & de Vaucouleurs (1986) formula relating bulge/disc ratio to galaxy morphology. As well as the large amount of scatter associated with this empirical formula, it is not clear that it is directly applicable to Seyfert galaxies. Indeed, if a typical early-type colour of $B - R_c = 1.6$ is assumed, then the bulge magnitudes adopted by Wandel correspond to an average of $M_R = -22.3 \pm 0.2$, half a magnitude brighter than the recent determination of M_R^* by Lin et al. (1996). In light of this it seems at least plausible that overestimation of the Seyfert galaxy bulge luminosities may contribute to the lower $M_{\text{bh}}/M_{\text{bulge}}$ ratios found by Wandel (1999).

In order to properly quantify the extent to which such overestimates of the Seyfert bulge luminosities can explain the Wandel (1999) result, it is important to obtain bulge luminosity estimates of comparable quality to those of the quasar sample. Suitable quality HST archive data is available for 9/15 of the Seyfert galaxies, predominantly from the large-scale Seyfert galaxy imaging study of Malkan, Gorjian & Tam (1998). The images of these objects were decomposed into disc and bulge components in an identical fashion to that utilised in the quasar host study of Dunlop et al. (2000), and details of the modelling technique used can be found in McLure, Dunlop & Kukula (2000). The remaining six Seyfert galaxies have bulge luminosity estimates taken from the disc/bulge decompositions of Baggett, Baggett & Anderson (1998) and Kotilainen, Ward & Williger (1993). Although determined from ground-based data, these published bulge luminosities are still expected to be more accurate than a morphology based estimate. The best estimates of the bulge luminosities for the quasar and Seyfert samples are listed in Tables 1 & 2 respectively.

4 THE BLACK-HOLE MASS VS. BULGE LUMINOSITY RELATION

The black-hole mass vs. bulge luminosity relation for the combined quasar and Seyfert galaxy sample is plotted in Fig 2. The two quantities can be seen to be well correlated, with the rank-order coefficient of $r_s = -0.66$ having a significance of 4.4σ . In order to obtain a reliable fit to the relation, a χ^2 minimization was used which properly accounts for the uncertainties in both the estimated black-hole masses and bulge luminosities (Press et al. 1992). The best-fitting relation ($\chi^2 = 64.8$ for 45 d.o.f.) is found to be:

$$\log(M_{\text{bh}}/M_\odot) = -0.61(\pm 0.08)M_R - 5.41(\pm 1.75) \quad (3)$$

and is shown as the solid line in the left-hand panel of Fig 2. In terms of black-hole mass the scatter around the best-fitting relation of $\sigma = 0.59$ is large (see Fig 3), although still comparable to that found by both Magorrian et al. (1998) and Laor (1998). In contrast to the findings of Wandel (1999) there is no evidence from Fig 2 that the Seyfert galaxy $M_{\text{bh}} - L_{\text{bulge}}$ relation is different to that of quasars. The removal of this discrepancy is due to the improved estimates of the Seyfert galaxy bulge luminosities used here. As mentioned in Section 3.2, it was suspected *a priori* that the bulge luminosities adopted by Wandel (1999) were probably overestimated. This suspicion is supported by the mean bulge luminosity derived for the Seyfert galaxies here, $M_R = -21.0 \pm 0.3$, which is 1.3 magnitudes fainter than estimated by Wandel (1999). It appears therefore that the evidence from this data-set supports a straightforward unification of Seyfert galaxies and quasars in which black-hole mass scales with bulge luminosity. In this scenario Fig 2 suggests that a black-hole mass of $\sim 10^{8.5} M_\odot$ needed to power a luminous quasar requires a host galaxy with a bulge luminosity of $M_R \sim -23$. This restriction naturally predicts that the hosts of luminous quasars will be predominantly massive early-type galaxies, in good agreement with the findings of recent studies (eg. McLure et al. 1999, Dunlop et al. 2000, Boyce et al. 1998).

4.1 Do black-hole and bulge mass scale linearly?

By combining bulge luminosity with a suitable mass-to-light ratio it is possible to test whether or not the observed $M_{\text{bh}} - L_{\text{host}}$ relation is consistent with a simple linear scaling between black-hole and bulge mass. The mass-to-light ratio adopted here is the $M/L \propto L^{0.31}$ relation determined by Jørgensen, Franx & Kjørgaard (1996), hereafter JFK96, from their Gunn- r fundamental plane study. Under the assumption that $M_{\text{bh}} = k M_{\text{bulge}}$, the $M_{\text{bh}} - L_{\text{host}}$ relation is expected to have the form:

$$\log(M_{\text{bh}}/M_\odot) = \log k - 0.52M_R - 0.66 \quad (4)$$

where the constant -0.66 results from assuming an average bulge colour of $M_r - M_{R_c} = 0.37$ (Fukugita et al. 1995) and an absolute Gunn- r magnitude for the Sun of $\simeq 4.65$ (Jørgensen 1994). A relation of this form, with a value of $k = 0.006$ as determined by Magorrian et al. (1998), is shown as the solid line in the right-hand panel of Fig 2. It can be seen that, for a given bulge luminosity adopting the Magorrian et al. normalization predicts black-hole masses approximately 2.5 times larger than determined via the H_β

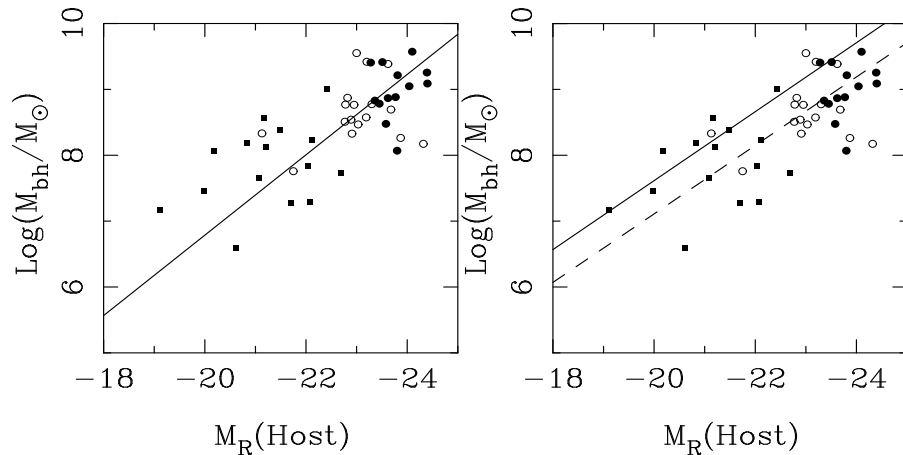


Figure 2. Both panels show black-hole mass vs. host galaxy R -band magnitude. The quasars which have black-hole masses estimated from the H_{β} FWHM and the $R_{\text{BLR}} - L_{5100}$ relation of Kaspi et al. (2000) are shown as open (radio quiet) and filled (radio loud) circles. The Seyfert galaxies from the sample of Wandel et al. (1999) which have black-hole estimates derived from reverberation mapping are shown as filled squares. In the left-hand panel the solid line is the best fit to the data. The solid line in the right-hand panel is the predicted relation from Magorrian et al. (1998) with $M_{\text{bh}}/M_{\text{bulge}} = 0.006$. The dashed line in the right-hand panel is best fit to the data forcing a constant $M_{\text{bh}}/M_{\text{bulge}}$ ratio, and corresponds to $M_{\text{bh}}/M_{\text{bulge}} = 0.0025$ (see text for discussion).

FWHM. It is also noteworthy however that the slope of -0.52 expected from a linear $M_{\text{bh}} - M_{\text{bulge}}$ relation is not inconsistent with the best-fitting value of -0.61 ± 0.08 determined above. Consequently, a least-squares fit of the data was undertaken with an enforced slope of -0.52 , and is shown as the dashed line in the right-hand panel of Fig 2. This can be seen to be a reasonable representation of the data, suggesting that the scaling between black-hole and bulge mass is consistent with being linear. The least-squares fit with an enforced slope of -0.52 has a intercept of -3.29 which, when compared with Equ 4, suggests that the constant of proportionality between black-hole and bulge mass is $k \simeq 0.0025$.

It is worth emphasising that this value for the constant of proportionality results, at least in part, from our use of a simple, but realistic disc-like model for the BLR, incorporating the known orientation biases of optically luminous AGN. If instead one simply uses the random orbit relation $V = \frac{\sqrt{3}}{2} \text{FWHM}$, then as discussed in Section 2, the inferred black-hole masses would be $\simeq 3$ times smaller, yielding the relation $M_{\text{bh}} = 0.0008 M_{\text{bulge}}$. This is the origin of the findings of Ho (1999) who studied the $M_{\text{bh}} - L_{\text{host}}$ relation in a sample 16 Seyfert galaxies (12 of which are common to the sample studied here) using published B -band photometry and virial black-hole mass estimates from reverberation mapping and H_{β} FWHM measurements. Ho found that the reverberation mapping black-hole estimates were lower than expected from the $M_{\text{bh}} - L_{\text{host}}$ relation, suggesting a value of $k \simeq 0.001$. Further evidence that simple random-orbit calculations for the BLR lead to systematic underestimation of black-hole mass is discussed in Section 5.

4.2 The ionizing continuum luminosity vs. bulge luminosity correlation

Fig 4 shows the correlation between bulge luminosity and continuum ionizing luminosity for the full sample, where we have adopted the relation $L_{\text{ion}} \simeq 10\lambda L_{5100}$ which was found to be the average of a large scatter by Wandel, Peterson

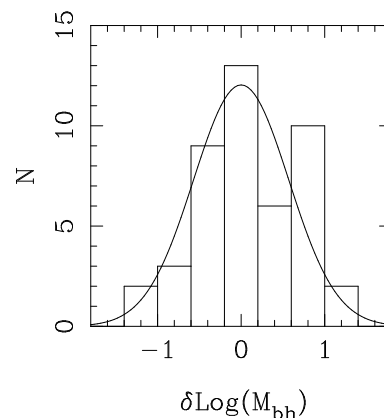


Figure 3. Histogram of the scatter around the best-fitting relation between black-hole mass and host galaxy magnitude. A gaussian with a standard deviation of $\sigma = 0.59$ is plotted for comparison.

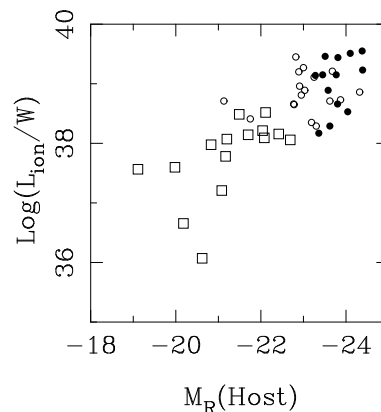


Figure 4. Ionizing continuum luminosity vs. host-galaxy R -band magnitude. The symbols are the same as Fig 2.

Source	z	M_R (bulge)	H_β FWHM	$\text{Log}(L_{\text{ion}}/W)$	$\text{Log}(M_{\text{bh}}/M_\odot)$	$L_{\text{ion}}/L_{\text{edd}}$
RLQ						
0137+012	0.258	-24.0 ± 0.20	7.61	38.53	9.05	0.03
0736+017	0.191	-23.6 ± 0.20	2.96	38.89	8.47	0.20
1004+130	0.240	-24.1 ± 0.75	6.34	39.51	9.57	0.07
1020-103	0.197	-23.4 ± 0.20	7.95	38.17	8.83	0.02
1217+023	0.240	-23.8 ± 0.20	3.83	39.15	8.88	0.14
1226+023	0.158	-24.4 ± 0.75	3.52	39.55	9.09	0.22
1302-102	0.286	-23.5 ± 0.75	3.40	39.15	8.78	0.18
1545+210	0.266	-23.3 ± 0.75	7.03	39.14	9.41	0.04
2135-147	0.200	-23.5 ± 0.20	5.50	39.46	9.42	0.09
2141+175	0.213	-23.8 ± 0.75	4.45	39.44	9.22	0.13
2247+140	0.237	-23.8 ± 0.20	2.22	38.66	8.07	0.30
2349-014	0.173	-24.4 ± 0.75	5.50	39.23	9.26	0.07
2355-082	0.210	-23.6 ± 0.20	7.51	38.29	8.87	0.02
RQQ						
0052+251	0.154	-23.0 ± 0.20	4.37	38.81	8.77	0.09
0054+144	0.171	-23.6 ± 0.20	9.66	38.71	9.39	0.02
0157+001	0.164	-24.3 ± 0.75	2.14	38.86	8.18	0.37
0204+292	0.109	-23.3 ± 0.20	1.04	38.29	8.78	0.03
0205+024	0.155	-21.1 ± 0.75	2.90	38.71	8.34	0.18
0244+194	0.176	-22.8 ± 0.20	3.70	38.66	8.51	0.11
0923+201	0.190	-23.3 ± 0.20	7.31	39.11	9.42	0.04
0953+414	0.239	-22.8 ± 0.20	2.96	39.45	8.87	0.29
1012+008	0.185	-23.9 ± 0.75	2.64	38.73	7.27	0.22
1029-140	0.086	-23.0 ± 0.75	7.50	39.27	9.55	0.04
1116+215	0.177	-23.7 ± 0.75	2.92	39.21	8.70	0.26
1202+281	0.165	-22.8 ± 0.75	5.01	38.65	8.77	0.06
1307+085	0.155	-22.9 ± 0.75	2.36	38.96	8.33	0.33
1309+355	0.184	-23.0 ± 0.75	2.94	38.89	8.47	0.20
1402+261	0.164	-21.8 ± 0.75	1.91	38.41	7.76	0.34
1444+407	0.267	-22.9 ± 0.75	2.48	39.20	8.54	0.35
1635+119	0.146	-23.2 ± 0.20	5.10	38.35	8.58	0.05

Table 1. Data for the quasar sample. Column three shows the host galaxy absolute R -band bulge magnitudes complete with estimated errors. Objects which are allocated an error of ± 0.2 magnitudes are all from the Dunlop et al. (2000) study. Objects which are allocated an error of ± 0.75 magnitudes are either highly morphologically disturbed objects from the Dunlop et al. study, or are taken from the Bahcall et al. (1997) study. Column four shows the FWHM of the H_β emission line in units of 1000 km s^{-1} . Column five lists the quasar ionizing luminosity, using the estimate that $L_{\text{ion}} \sim 10\lambda L_{5100}$. Column six lists the black-hole masses in solar units as derived from the H_β FWHM and 5100 \AA continuum luminosity (see text). Column seven lists the quasar ionizing luminosity as a fraction of the Eddington luminosity.

& Malkan (1999). These two quantities are well correlated ($r_s = -0.73, 4.85\sigma$), in apparent agreement with the results of the combined Seyfert galaxy and quasar study of McLeod & Rieke (1995). McLeod & Rieke found a relation between H -band host luminosity and B -band nuclear luminosity in the form of a lower limit, such that $M_H(\text{host}) \geq M_B(\text{nucleus})$.

However, it is also noticeable from Fig 4 that the correlation between L_{ion} and L_{host} is entirely dependent upon the low luminosity Seyfert galaxies, with the quasar sample on its own displaying no significant correlation, $r_s = 0.27, 1.45\sigma$. The conclusion that the correlation between L_{ion} and L_{host} breaks down at higher nuclear luminosities is supported by the results of a study of high-luminosity quasars by Percival et al. (2000). Although including quasars up to a factor of ten more luminous than those studied here, Percival et al. find very similar host galaxy luminosities. The suggestion is therefore that high luminosity quasars operate at higher accretion rates, rather than harbouring significantly more massive black-holes.

The correlation between L_{ion} and L_{host} amongst the

Seyfert galaxies raises the possibility that the observed correlation between M_{bh} and L_{host} could in fact be simply due to independent correlations with L_{ion} . In order to investigate this possibility the partial Spearman rank correlation test (Macklin 1982) has been used to quantify the correlation between M_{bh} and L_{host} , independent of L_{ion} . The correlation between M_{bh} and L_{host} at constant L_{ion} has a coefficient of $r_s = -0.28$ which has a significance of 1.9σ . Therefore, although the M_{bh} and L_{host} correlation is still clearly present, its significance is substantially lowered.

Unfortunately, due to the heterogeneous nature of the sample of Seyfert galaxies which currently have reverberation mapping data available, it is difficult to quantify properly the significance of the $M_{\text{bh}} - L_{\text{host}}$ relation. In order to overcome this problem, a substantially larger sample of AGN is required, selected from a narrow slice in both nuclear luminosity and redshift.

Source	z	$M_R(\text{bulge})$	$\text{Log}(M_{\text{bh}}/M_{\odot})$	Bulge luminosity details
IC 4329A	0.016	-19.11 ± 1.00	7.18	B/D decomposition from Kotilainen, Ward & Williger (1993)
Fairall 9	0.047	-21.49 ± 1.00	8.38	B/D decomposition from Kotilainen, Ward & Williger (1993)
3C 120	0.033	-22.04 ± 0.75	7.84	This work, HST archive image, PID=6285, Filter=F675W
3C 390.3	0.056	-22.42 ± 0.75	9.01	This work, HST archive image, PID=5476, Filter=F702W
Mrk 79	0.022	-20.83 ± 0.75	8.20	This work, HST archive image, PID=5479, Filter=F606W
Mrk 335	0.026	-21.70 ± 0.75	7.18	This work, HST archive image, PID=5479, Filter=F606W
Mrk 509	0.034	-22.11 ± 1.00	8.24	B/D decomposition from Kotilainen, Ward & Williger (1993)
Mrk 590	0.026	-22.69 ± 0.75	7.73	This work, HST archive image, PID=5479, Filter=F606W
Mrk 817	0.032	-21.20 ± 0.75	8.12	This work, HST archive image, PID=5479, Filter=F606W
NGC 3227	0.004	-19.38 ± 1.00	8.07	B/D decomposition from Baggett, Baggett & Anderson (1998)
NGC 3783	0.010	-19.85 ± 0.75	7.45	This work, HST archive image, PID=5479, Filter=F606W
NGC 4051	0.002	-20.62 ± 1.00	6.59	B/D decomposition from Baggett, Baggett & Anderson (1998)
NGC 4151	0.003	-19.05 ± 1.00	7.66	B/D decomposition from Baggett, Baggett & Anderson (1998)
NGC 5548	0.017	-21.17 ± 0.75	8.57	This work, HST archive image, PID=5479, Filter=F606W
NGC 7469	0.016	-22.08 ± 0.75	7.29	This work, HST archive image, PID=5479, Filter=F606W

Table 2. Data for the Seyfert galaxy sample. Column three shows the absolute R -band bulge magnitudes complete with estimated errors. Objects whose host galaxies have been modelled for this paper have been allocated an error of ± 0.75 magnitudes. Objects whose bulge luminosity has been taken from the literature have been allocated an error of ± 1.0 magnitudes. Column four shows the virial black-hole mass estimates based on reverberation mapping and mean H_{β} FWHM measurements from Kaspi et al. (2000) and the disc model of the BLR discussed in the text. Column 5 gives details of how the bulge luminosities were determined. For those objects for which we present new bulge/disc decompositions from HST archive data we have also listed the ID number of the HST proposal from which the data were taken.

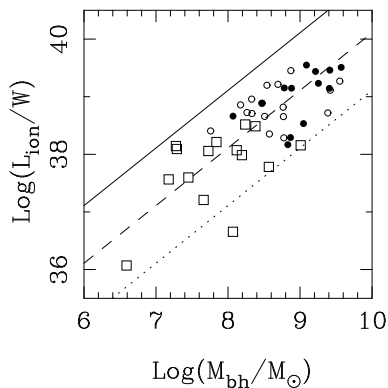


Figure 5. Ionizing continuum luminosity vs. black-hole mass. The three lines indicate the location of objects radiating with a luminosity equal to L_{Edd} (solid), $0.1L_{\text{Edd}}$ (dashed) and $0.01L_{\text{Edd}}$ (dotted). The symbols are the same as Fig 2.

4.3 Black-hole mass and unification

The black-hole mass estimates for the 17 radio-quiet and 13 radio-loud quasars studied here provide an opportunity to determine the influence (if any) of black-hole mass on quasar radio luminosity. The ionizing continuum luminosity distributions of the two quasar sub-samples are indistinguishable, with a Kolmogorov-Smirnov (KS) test returning a probability of $p = 0.18$ that both sub-samples are drawn from the same underlying distribution. Consequently, any difference in the distribution of black-hole masses between the two sub-samples is presumably linked to the difference in radio properties.

With the results of Section 4.1 showing that AGN black-hole and bulge masses are consistent with being directly proportional, it is expected that the 0.77 magnitude difference in median bulge luminosity between the quasar sub-samples

should translate directly into a corresponding difference in average black-hole mass. This is indeed the case, with the median black-hole mass of the radio-loud sub-sample a factor of three larger than that of the radio-quiet sub-sample. A natural division between the quasar sub-samples appears to occur at $M_{\text{bh}} \sim 10^{8.8} M_{\odot}$. Only 2/13 of the radio-loud quasars have $M_{\text{bh}} < 10^{8.8} M_{\odot}$, while only 4/17 of the radio-quiet have $M_{\text{bh}} > 10^{8.8} M_{\odot}$. This difference in black-hole mass distributions is shown to be significant at the 2.9σ ($p = 0.004$) level by a KS test. The implication from the quasar sample is therefore that (albeit with substantial overlap) for a given nuclear luminosity, the probability of a source being radio-loud increases with black-hole mass, or alternately decreases with $L_{\text{ion}}/L_{\text{Edd}}$.

Fig 5 shows a plot of estimated ionizing luminosity vs. black-hole mass, together with lines indicating the location of objects radiating at 100%, 10% and 1% of the Eddington limit. Two aspects of this figure are noteworthy. Firstly, it can be seen that the vast majority of the objects appear to be radiating in the range $5 \rightarrow 30\%$ of the Eddington limit, with a mean value of $L_{\text{ion}}/L_{\text{Edd}} = 0.15$. This is despite the fact that the sample spans a range in ionizing luminosity of four orders of magnitude, and is in contrast to the results of Wandel, Peterson & Malkan (1999) and Kaspi et al. (2000) who both find that the $L_{\text{ion}}/L_{\text{Edd}}$ ratio increases weakly with continuum luminosity. Secondly, there appears to be no evidence that the Seyfert galaxies are operating in a different accretion regime to the quasars, contrary to the finding of Lu & Yu (1999). However, it should also perhaps be noted that differences between the UV spectra of Seyfert galaxies and quasars could well mean that a global correction of the form $L_{\text{ion}} = 10\lambda L_{5100}$ is inappropriate.

5 THE NORMALIZATION OF THE $M_{\text{bh}} - M_{\text{bulge}}$ RELATION

In this section the possibility of calibrating the virial H_{β} FWHM black-hole estimates, by taking advantage of the remarkably small scatter in the recently discovered $M_{\text{bh}} - \sigma$ correlation, is explored. Considering that H_{β} FWHM measurements can be obtained with relative ease for powerful AGN, in comparison with determining the host-galaxy stellar velocity dispersion, this is a question of some interest.

Although stellar velocity measurements are not available for the quasar sample, a comparison is still possible for the 19 objects which are taken from the host-galaxy study of McLure et al. (1999) and Dunlop et al. (2000). One of the main successes of this study was the first demonstration that the massive elliptical host galaxies of these quasars follow an identical Kormendy relation ($\mu_e - r_e$) to normal inactive ellipticals. Therefore, because the Kormendy relation is simply a projection of the fundamental plane that elliptical galaxies occupy in the three dimensional space defined by (r_e, σ, I_e), it is possible to use the r_e & I_e data for these objects to estimate their stellar velocity dispersions. The fundamental plane parameters adopted here are those determined for the Coma cluster by JFK96:

$$\log r_e = 1.31 \log \sigma - 0.84 \log \langle I \rangle_e - 0.0082 \quad (5)$$

Although there is evidence that the form of the fundamental plane changes with redshift, the form of this evolution ($\Delta \log(M/L) = -0.26 \Delta z$; Jørgensen et al. 1999) should not introduce significant errors at the average redshift of the quasar sample ($z \simeq 0.2$).

Due to the disagreement over what the correct form of the $M_{\text{bh}} - \sigma$ relation is, both the $M_{\text{bh}} \propto \sigma^{3.75}$ (Gebhardt et al. 2000a) and $M_{\text{bh}} \propto \sigma^{4.72}$ (Merritt & Ferrarese 2000) versions of the relation have been used to convert the velocity dispersion estimates into black-hole masses. In both cases the $M_{\text{bh}} - \sigma$ relations predict black-hole masses which are in remarkably good agreement with our virial H_{β} estimates, with median $M_{\text{bh}}(\sigma)/M_{\text{bh}}(H_{\beta})$ ratios of 1.04 & 1.31 for the Gebhardt et al. and Merritt & Ferrarese relations respectively. The clear implication of this comparison is that the use of a disc-like BLR, combined with limits of disc orientation relative to the observer, has led to reliable virial H_{β} FWHM estimates of black-hole mass. In contrast, the standard assumption of purely random BLR velocities lead to virial H_{β} FWHM black-hole mass estimates which appear to be systematically low by a factor of $2 \rightarrow 3$.

A similar systematic problem with the assumption of random orbits was alluded to by Gebhardt et al. (2000b) when they compared (random orbit) virial black-hole mass estimates, based on reverberation mapping and H_{β} FWHM measurements, with velocity dispersion black-hole masses for a sample of seven Seyfert galaxies (five of which are common to the sample studied here). Although Gebhardt et al. (2000b) concluded that the discrepancy between the two black-hole mass estimates was not significant, they did comment that an increase in the reverberation mapping estimates by a factor of $\simeq 2$ would improve the agreement.

Finally, in further support of the relation $M_{\text{bh}} \simeq 0.0025 M_{\text{bulge}}$ derived from our H_{β} FWHM analysis, we note that Gebhardt et al. (2000b) also comment that new three integral models show that the black-hole masses originally

determined by Magorrian et al. (1998) were overestimated by a factor of ~ 3 , again leading to the conclusion that $M_{\text{bh}} \sim 0.002 M_{\text{bulge}}$.

6 CONCLUSIONS

The black-hole masses for a sample of 30 optically-matched radio-loud and radio-quiet quasars have been estimated using H_{β} FWHM and continuum luminosity measurements from new and previously published nuclear spectra. Reliable quasar bulge luminosities have been combined with new and published disc/bulge decompositions for a sample of Seyfert galaxies with reverberation mapping black-hole estimates, in order to study the form of the $M_{\text{bh}} - L_{\text{host}}$ relation over a large baseline in AGN luminosity. The results of the H_{β} black-holes mass estimates have been compared with the $M_{\text{bh}} - \sigma$ correlation in an attempt to check the normalization of the $M_{\text{bh}} - M_{\text{bulge}}$ relation. The main conclusions of this study can be summarized as follows:

(i) Host-galaxy bulge luminosity and black-hole mass are found to be well correlated, albeit with scatter of 0.6 dex in M_{bh} . Assuming a simple but realistic disc-like geometry for the BLR, coupled with limits on viewing angle for optically-luminous AGN, the form of the $L_{\text{host}} - M_{\text{bh}}$ correlation is shown to be consistent with $M_{\text{bh}} \simeq 0.0025 M_{\text{bulge}}$.

(ii) Contrary to the results of Wandel (1999) no evidence is found that Seyfert galaxies follow a different $M_{\text{bh}} - L_{\text{host}}$ relation to quasars. The results presented here suggest that unification of Seyfert galaxies and radio-quiet quasars via a simple scaling in black-hole mass is tenable.

(iii) A comparison of the virial black-hole estimates based on H_{β} FWHM measurements with those predicted by the $M_{\text{bh}} - \sigma$ relation suggests that our H_{β} black-hole estimates are, on average, accurate to within a factor < 1.5 . These two, completely independent approaches to black-hole mass estimation both support a black-hole mass vs. bulge mass relation of the form $M_{\text{bh}} \simeq 0.0025 M_{\text{bulge}}$.

(iv) The distribution of black-hole masses in the radio-quiet and radio-loud quasar sub-samples are found to be significantly different ($p = 0.004$), with the median radio-loud black-hole mass a factor of three larger than the equivalent radio-quiet value. It appears that, for some reason, a radio-loud quasar requires a black-hole mass $> 6 \times 10^8 M_{\odot}$.

Finally, perhaps the most important conclusion resulting from this study is that easily obtainable AGN nuclear spectra can be used to provide black-hole mass estimates which are accurate to within a factor of < 2 . It is therefore possible that large-scale studies of AGN black-hole demography can be undertaken without the need for more demanding and time-intensive stellar velocity dispersion measurements.

7 ACKNOWLEDGEMENTS

The INT is operated on the island of La Palma by the Isaac Newton Group in the Spanish Observatorio del Roque de los Muchachos of the Instituto de Astrofísica de Canarias. Based on observations with the NASA/ESA Hubble Space Telescope, obtained at the Space Telescope Science Institute,

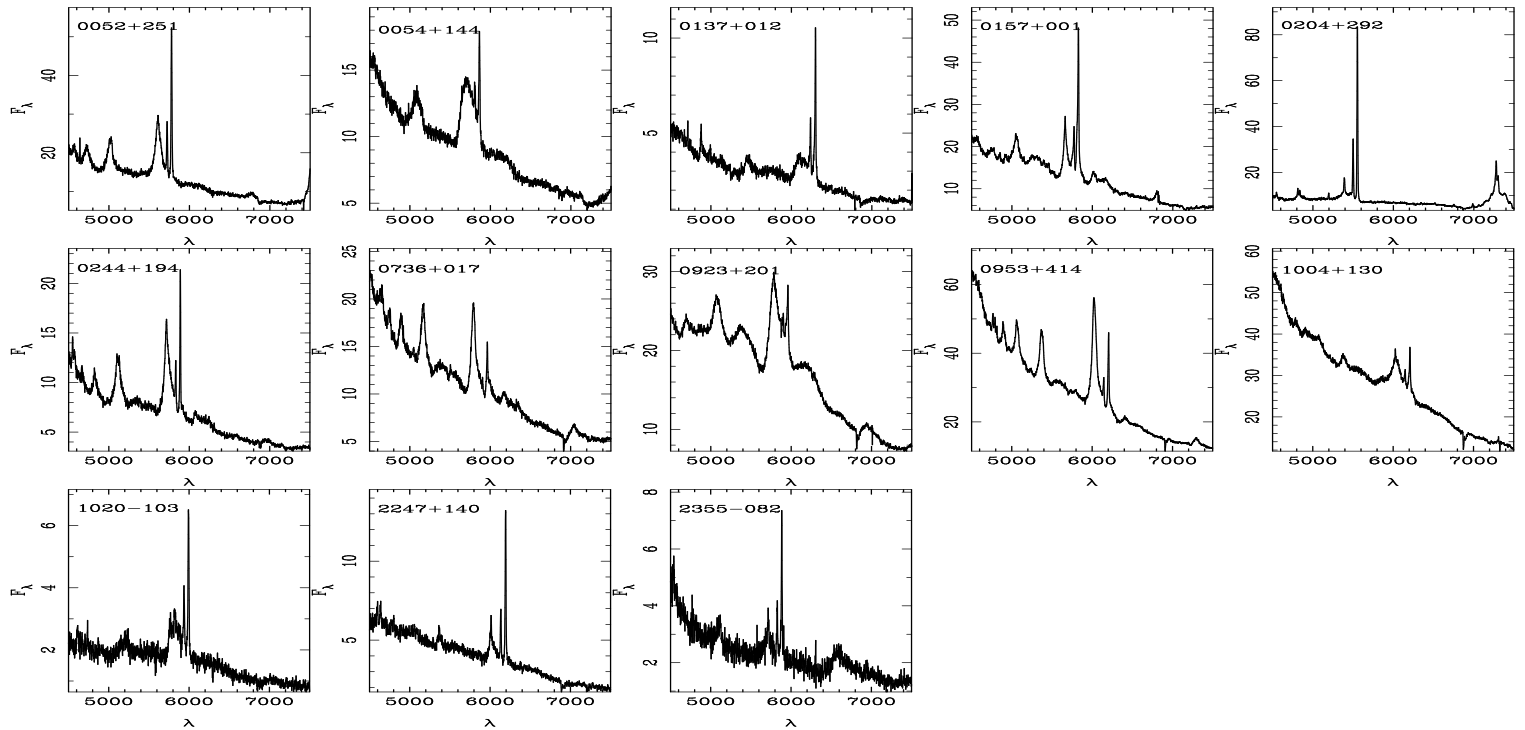


Figure 6. The final reduced quasar spectra obtained with IDS on the Isaac Newton Telescope. The spectra are displayed in the observed frame with wavelength in Angstroms. The vertical axis shows object flux in units of $10^{-16} \text{ergs cm}^{-2} \text{s}^{-1} \text{\AA}^{-1}$. Object names are displayed in the top left-hand corner of each individual spectrum.

which is operated by the Association of Universities for Research in Astronomy, Inc. under NASA contract No. NAS5-26555. This research has made use of the NASA/IPAC Extragalactic Database (NED) which is operated by the Jet Propulsion Laboratory, California Institute of Technology, under contract with the National Aeronautics and Space Administration. RJM acknowledges a PPARC PDF.

8 REFERENCES

- Antonucci R., Miller J.S., 1985, *ApJ*, 297, 621
 Baggett W.E., Baggett S.M., Anderson K.S.J., 1998, *AJ*, 116, 1626
 Bahcall J.N., Kirhakos S., Saxe D.H., Schneider D.P., 1997, *ApJ*, 479, 642
 Boroson T.A., Green R.F., 1992, *ApJS*, 80, 109
 Boyce P.J., et al., 1998, *MNRAS*, 298, 121
 Corbin M.R., 1997, *ApJS*, 113, 245
 Dunlop J.S., et al., 2001, *MNRAS*, submitted,
 Fukugita M., Shimasaku K., Ichikawa T., 1995, *PASP*, 107, 945
 Gebhardt K., et al., 2000a, *ApJ*, 539, L13
 Gebhardt K., et al., 2000b, *ApJ*, 543, L5
 Ho, L.C., 1999, in Chakrabarti S.K., ed, *Proc Observation evidence for the black holes in the universe*, Kluwer, Dordrecht, p.157
 Jørgensen I., 1994, *PASP*, 106, 967
 Jørgensen I., Franx M., Kjaergaard P., 1996, *MNRAS*, 280, 167
 Jørgensen I., Franx M., Hjorth J., van Dokkum P.G., 1999, *MNRAS*, 308, 833
 Kaspi S., Smith P.S., Netzer H., Maoz D., Jannuzi B.T., Giveon U., 2000, *ApJ*, 533, 631
 Kauffmann G., Haehnelt M., 2000, *MNRAS*, 311, 576
 Kormendy J., Richstone D., 1995, *ARA&A*, 33, 581
 Kotilainen J.K., Ward M.J., Williger, 1993, *MNRAS*, 263, 655
 Laor A., 1998, *ApJ*, 505, L83
 Lin H., Kirshner P.P., Schectman S.A., Landy S.D., Oemler A., Tucker Lu Y., Yu Q., *ApJ*, 1999, 526, L5
 D.L., Schechter P.L., 1996, *ApJ*, 464, 60
 Macklin J.T., 1982, *MNRAS*, 199, 1119
 McLeod K.K., Rieke G.H., 1995, *ApJ*, 441, 96
 McLure R.J., Dunlop J.S., Kukula M.J., Baum S.A., O’Dea C.P., Hughes D.H., 1999, *MNRAS*, 308, 377
 McLure R.J., Dunlop J.S., Kukula M.J., 2000, *MNRAS*, 318, 693
 Magorrian J., et al., 1998, *AJ*, 115, 2285
 Malkan M., Gorjian V., Tam R., 1998, *ApJS*, 117, 25
 Merritt D., Ferrarese L., 2000, *MNRAS*, 2001, 320, L30
 Percival W.J., Miller L., McLure R.J., Dunlop J.S., 2000, *MNRAS*, in press, astro-ph/0002199
 Press W.H., Teukolsky S.A., Vetterling W.T., Flannery B.P., 1992, *Numerical Recipes*, Cambridge University Press
 Schade D.J., Boyle B.J., Letawsky M., 2000, *MNRAS*, 315, 498
 Silk J., Rees M.J., 1998, *A&A*, 331, L1
 Simien F., de Vaucouleurs G., 1986, *ApJ*, 302, 564
 van der Marel, R.P., 1999, in Barnes J.E., Sanders D.B., eds, *Proc IAU Symp. 186, Galaxy interactions at low and high redshift*, Kluwer, Dordrecht, p. 333
 Vestergaard M., Wilkes B.J., Barthel P.D., 2000, *ApJ*, L103

Wandel A., 1999, ApJ, 519, L39

Wandel A., Peterson B.M., Malkan M.A., 1999, ApJ, 526, 579

Wang Y.P., Biermann P.L., Wandel A., 2000, A&A, in press, astro-ph/0008105

Wills B.J., Browne I.W.A., 1986, ApJ, 302, 56

Wilman R.J., Fabian A.C., Nulsen P.E.J., 2000, MNRAS, in press, astro-ph/0008019

Whittle M., 1992, ApJS, 79, 49